Modelling the dense nuclear matter equation of state consistent with the astrophysical observations

Prasanta Char
Space sciences, Technologies and Astrophysics Research (STAR) Institute, University of Liège

Advances in Astroparticle Physics and Cosmology (AAPCOS-2023)

NS Structure

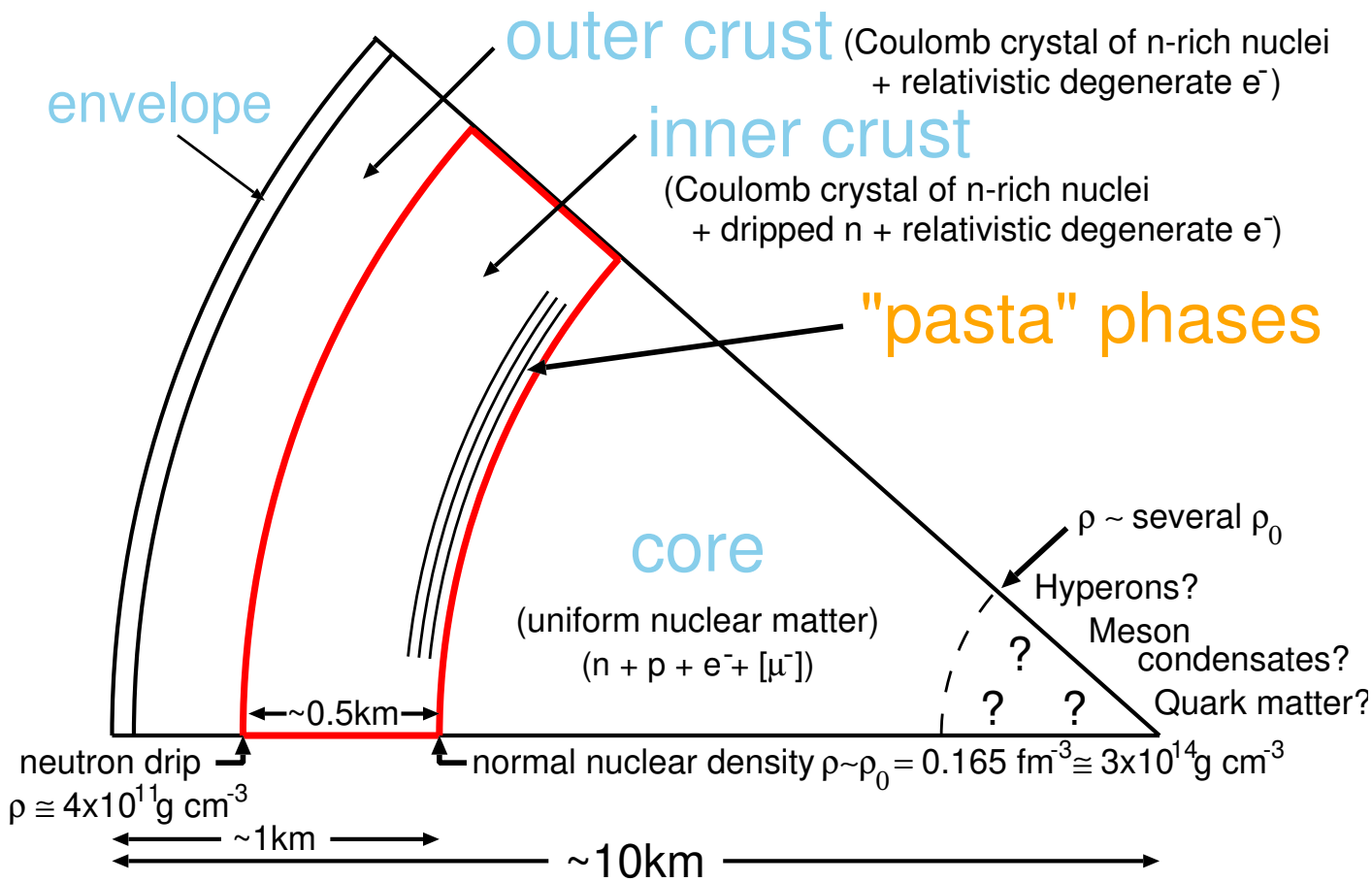

Figure: **Schematic picture of a NS Interior**

Equation of State and Mass-Radius

$P = P(\rho)$ ⟷ $M = M(R)$

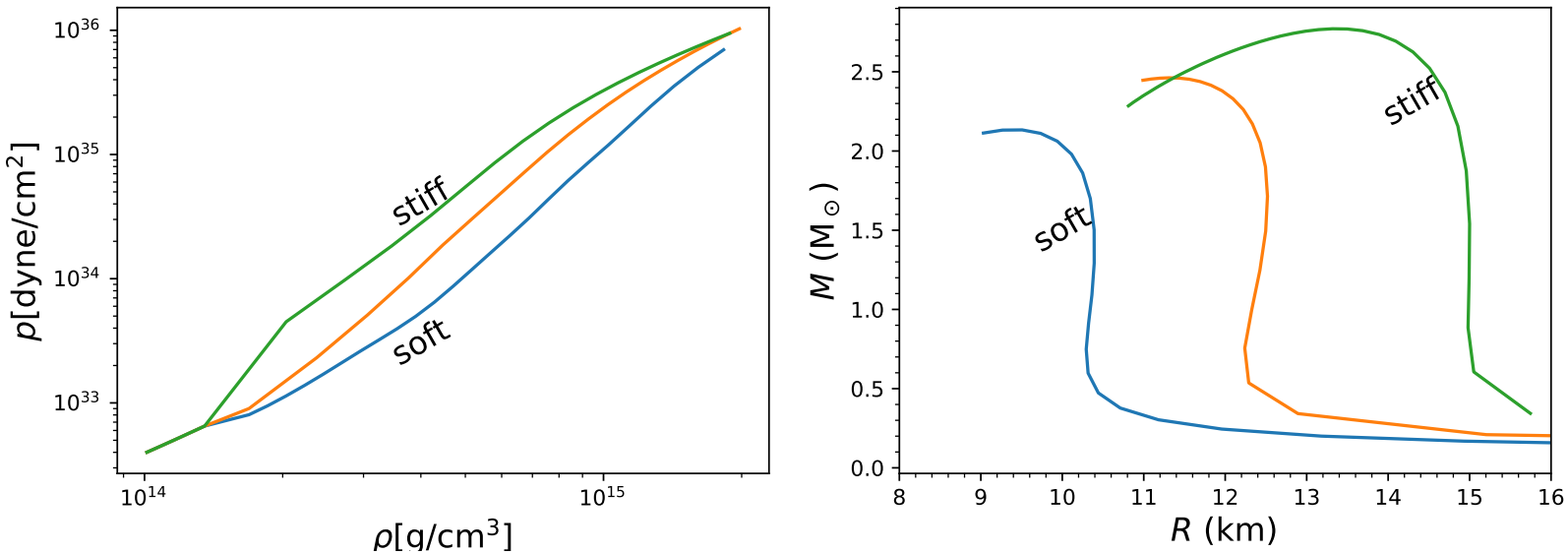

One to one correspondence between Equation of State (EOS) and mass-radius

Tidally Deformed Stars

- If a static spherically symmetric star of mass M and radius R is placed in a time-independent external tidal field $\mathcal{E}_{ij}$, a quadrupole moment Q_{ij} is induced onto the star and to linear order

$$Q_{ij} = -\lambda \mathcal{E}_{ij},$$

- Tidal deformation parameter λ related to the $l = 2$ dimensionless Love number k_2

$$\lambda = \frac{2}{3} k_2 R^5.$$

- Observational parameter in LIGO: $\Lambda = \lambda / M^5$

Saturation properties of nuclear matter:

Paremeters are obtained by fitting to the saturation properties of nuclear matter:

- Binding energy: $E/A \simeq -16$ MeV.
- Saturation density: $\rho_0 \simeq 0.16$ fm^{-3}
- Effective mass of nucleons: ~ 0.7
- Incompressibility: $K = 210 - 280$ MeV
- Symmetry energy: $J = 28 - 35$ MeV.
- Symmetry energy slope : $L = 30 - 87$ MeV

Margueron et al., PRC 97, 025805 (2018)

NS Observations that an EOS must satisfy

- Precise mass-measurements of massive NSs:

  $(1.908 \pm 0.016) M_\odot$ Arzoumanian et al, ApJS 235, 37 (2018).

  $(2.01 \pm 0.04) M_\odot$ Antoniadis et al, Science 340, 448 (2013).

  $(2.08 \pm 0.07) M_\odot$ E. Fonseca et al, ApJL 915 L12 (2021).

- BNS merger event GW170817 provides bounds on tidal deformability (Λ), and pressure at $2\rho_0$; Abbott et al, PRL 121, 161101 (2018):

  $\Lambda_{1.4} = 190^{+390}_{-120} \Rightarrow \Lambda_{1.4} \leq 580$, $P(2\rho_0) = 3.5^{+2.7}_{-1.7} \times 10^{34}$ dyn/cm^2

- NICER collaboration provided:

  1) Simultaneous mass-radius measurements of PSR J0030+0451

  $M = 1.34^{+0.15}_{-0.16} M_\odot$, $R = 12.71^{+1.14}_{-1.19}$km Riley et al, ApJL, 887, L21 (2019).

  $M = 1.44^{+0.15}_{-0.14} M_\odot$, $R = 13.02^{+1.24}_{-1.06}$km Miller et al, ApJL, 887, L24 (2019).

  2) Radius measurements of J0740+6620

  $R = 12.39^{+1.30}_{-0.98}$km Riley et al., ApJL, 918, L27 (2021).

  $R = 13.7^{+2.6}_{-1.5}$km Miller et al., ApJL, 918, L28 (2021).

Relativistic Mean Field Theory

- Interaction between baryons is described via exchange of mesons.
- The most general form of the interaction Lagrangian density:

$$
\begin{aligned}
\mathcal{L}_{\rm int} \;=\; & \sum_B \bar{\psi}_B \left[g_\sigma \sigma + g_\delta \; \boldsymbol{\tau}\cdot\boldsymbol{\delta} - \gamma^\mu \left(g_\omega \omega_\mu + \frac{1}{2} g_\rho \boldsymbol{\tau}\cdot\boldsymbol{\rho_\mu} + \frac{e}{2}(1+\tau_3) A_\mu \right) \right] \psi_B \\
& - \frac{\kappa}{3!}(g_\sigma \sigma)^3 - \frac{\lambda}{4!}(g_\sigma \sigma)^4 + \frac{\zeta}{4!}(g_\omega^2 \omega_\mu \omega^\mu)^2 \\
& + g_\sigma g_\omega^2 \sigma \omega_\mu \omega^\mu \left(\alpha_1 + \frac{1}{2}\alpha_1' g_\sigma \sigma \right) + g_\sigma g_\rho^2 \sigma \boldsymbol{\rho_\mu}\cdot\boldsymbol{\rho^\mu} \left(\alpha_2 + \frac{1}{2}\alpha_2' g_\sigma \sigma \right) \\
& + \frac{1}{2}\alpha_3' g_\omega^2 g_\rho^2 \omega_\mu \omega^\mu \; \boldsymbol{\rho_\mu}\cdot\boldsymbol{\rho^\mu}
\end{aligned}
$$

  σ, ω_μ, $\boldsymbol{\rho_\mu}$ and $\boldsymbol{\delta}$ are meson fields.

- For density dependent (DD) models coupling parameters g_σ, g_ω, g_ρ and g_δ are density dependent and don't have nonlinear terms.

Based on the form of interaction Lagrangian density we group the models in several classes:

Name	Type of interaction for mesons
NL	σ SI
S271	σ SI + (ω, ρ) CC
NL3 family	σ SI + (σ, ρ) or (ω, ρ) CC
FSU family	σ SI + ω SI + (ω, ρ) CC
Z271 family	σ SI + ω SI + (σ, ρ) or (ω, ρ) CC
BSR family	σ SI + all possible (σ, ω), (σ, ρ) and (ω, ρ) CCs
BSR* family	σ SI + ω SI + all possible (σ, ω), (σ, ρ) and (ω, ρ) CCs
DD	density-dependent couplings

SI = self-interaction, CC=cross-coupling

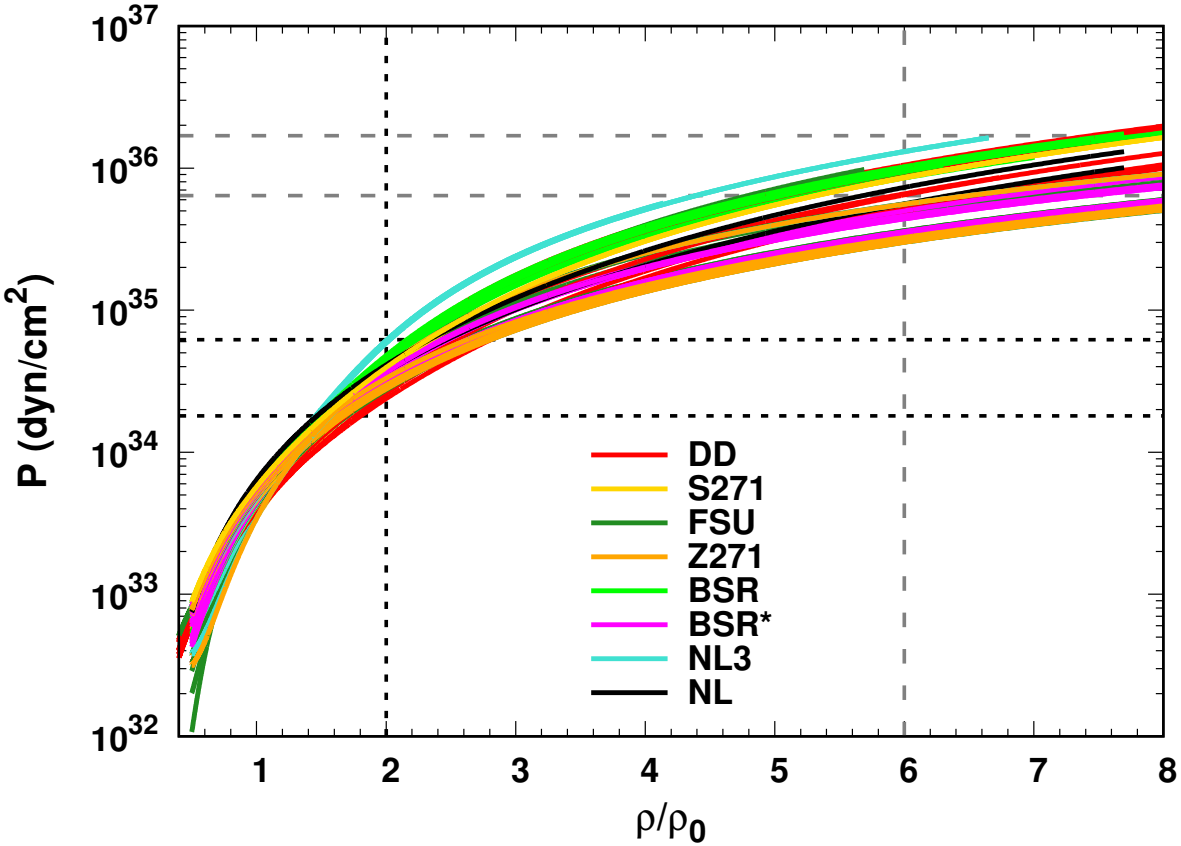

Figure: Pressure vs normalized baryon density for collected RMF parameter sets from Dutra et al. PRC 90, 055203 (2014)

GW170817 bounds

$$P(2\rho_0) = 3.5^{+2.7}_{-1.7} \times 10^{34}\ \mathrm{dyn/cm^2}, \quad P(6\rho_0) = 9.0^{+2.6}_{-7.9} \times 10^{35}\ \mathrm{dyn/cm^2}$$

$\Rightarrow$ All EOS satisfy the $P(2\rho_0)$ constraint.

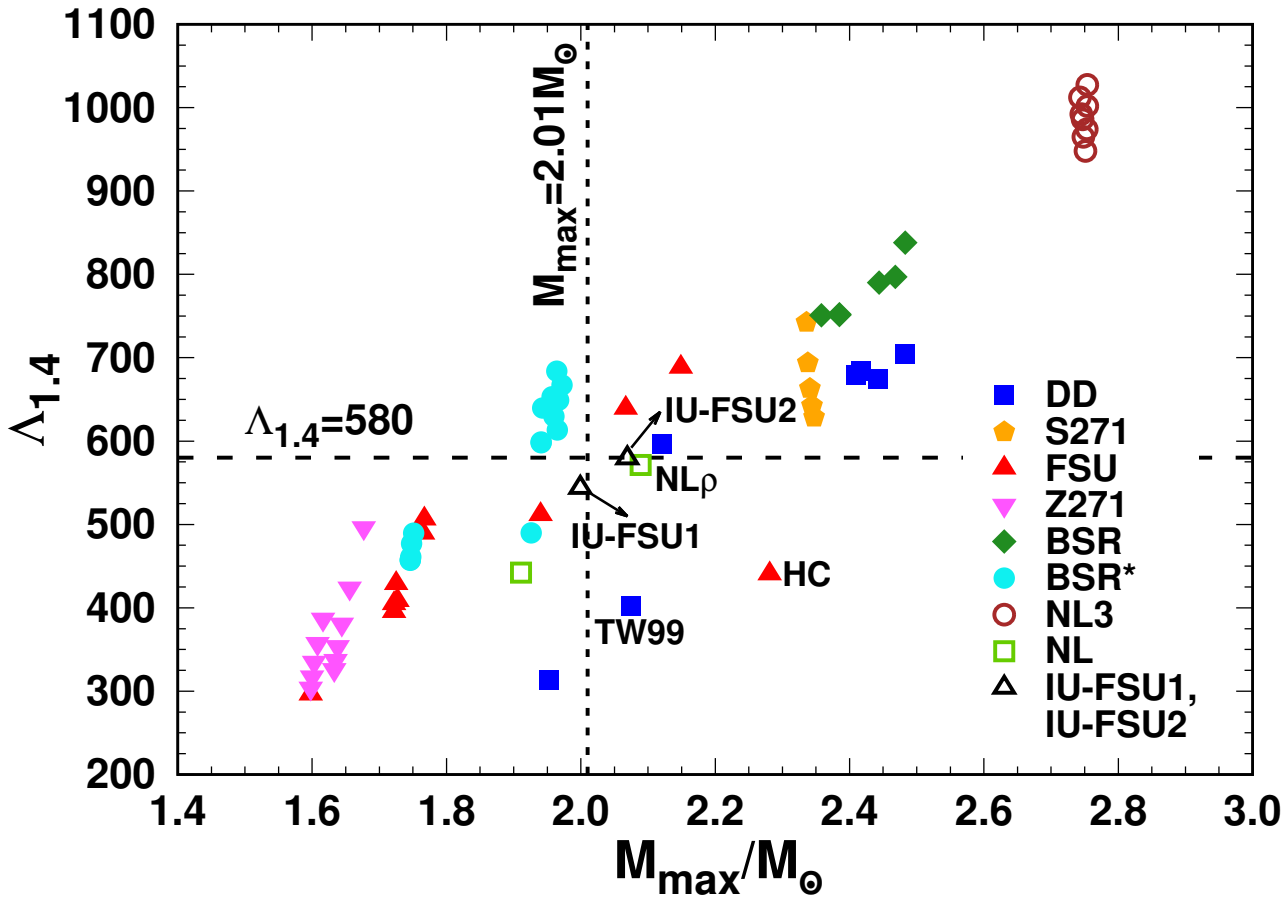

$M_{\rm max}$ constraint	GW170817 bound
$M_{\rm max} = 2.08 \pm 0.07 M_\odot$	$\Lambda_{1.4} = 190^{+390}_{-120}$
i.e. $M_{\rm max} \geq 2.01 M_\odot$	$\Lambda_{1.4} \leq 580$

$\Rightarrow$ Only 3 EOS (TW99, NLρ and HC) satisfy both the constraints

M-R Diagram

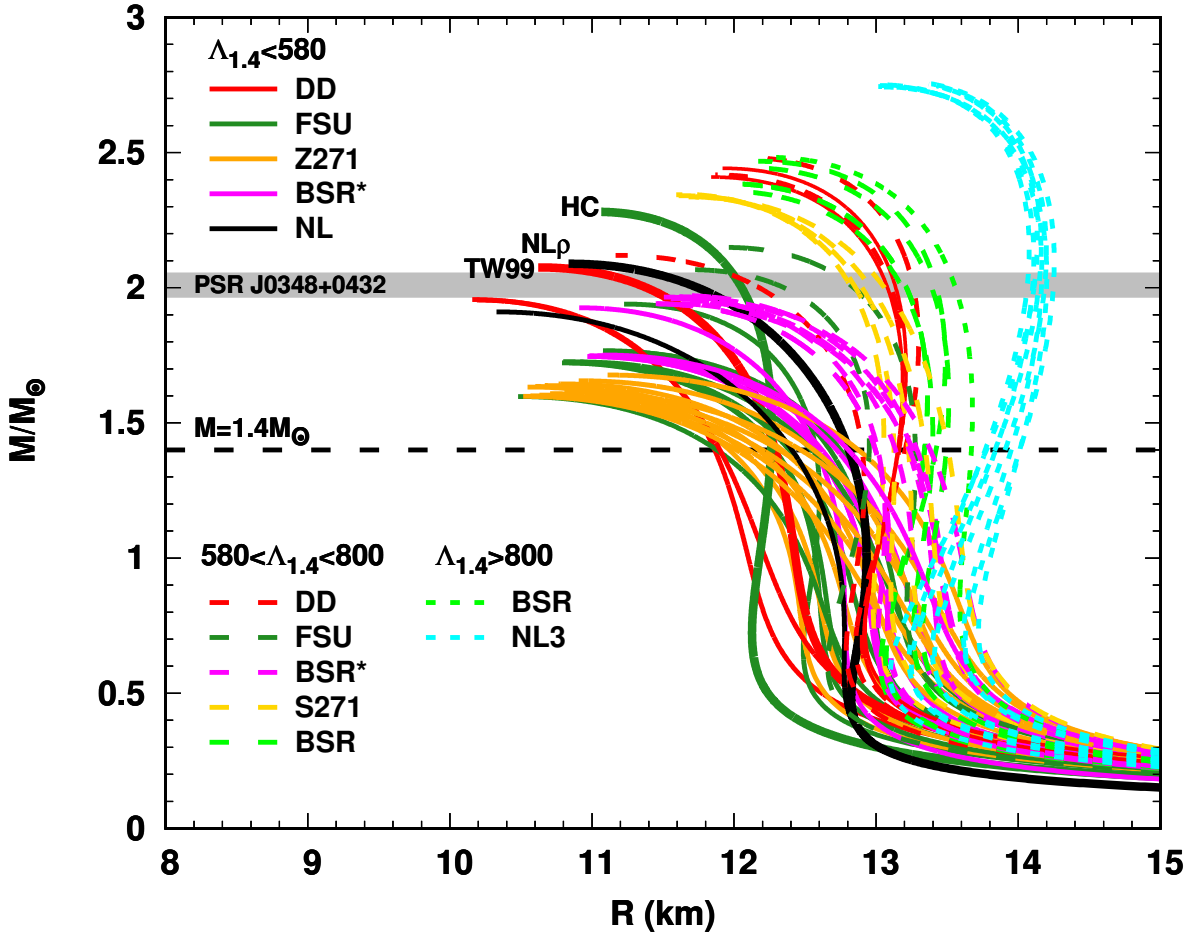

$\Rightarrow R_{1.4} < 12.9$ km

R. Nandi, P.C., S. Pal; PRC 99, 052802(R) (2019)

Neutron skin thickness

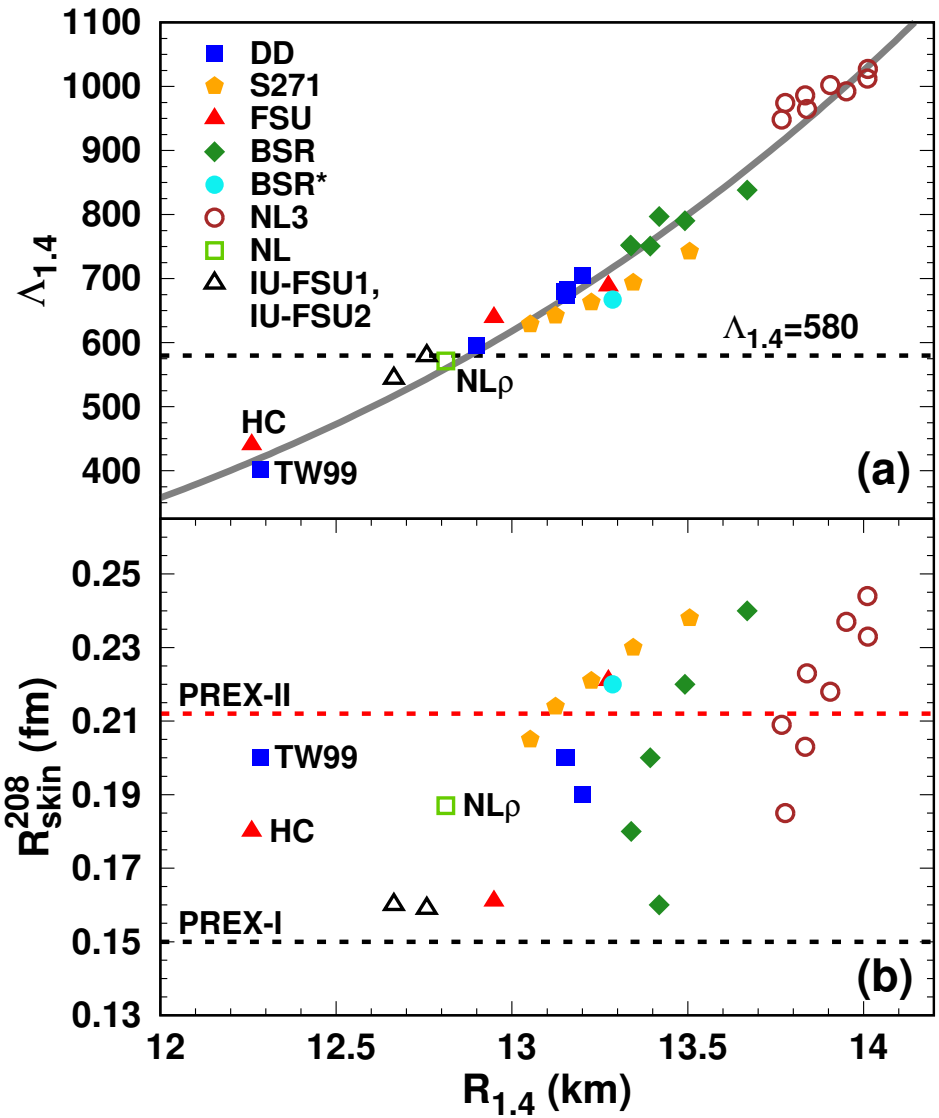

R. Nandi, P.C., S. Pal; PRC 99, 052802(R) (2019)

$R_{1.4} \lesssim 12.9$ km,

$R_{\rm skin} = < r_n > - < r_p >$

- PREX-I:
  $R^{208}_{\rm skin} = 0.33^{+0.16}_{-0.18}$ fm
  PRL 108, 112502(2012)
- PREX-II:
  $R^{208}_{\rm skin} = 0.28 \pm 0.07$ fm
  PRL 126, 172502(2021)

Including hyperons

Model	$M_{\rm max}/M_\odot$	$R_{1.4}$(km)	$n_{1.4}$(fm^{-3})	$n_{\rm th}$(fm^{-3})	$\Lambda_{1.4}$
S271v6	2.35	13.05	0.375		626
with Hyperons	1.89	13.05	0.375	0.376	
BSR3	2.36	13.40	0.348		747
with Hyperons	1.90	13.39	0.355	0.336	
DD2	2.42	13.160	0.353		683
with Hyperons	2.10	13.156	0.361	0.331	681

Hyperon-meson couplings are obtianed from SU(6) model and considering $U_\Lambda^{(N)} = -28$ MeV, $U_\Sigma^{(N)} = 30$ MeV and $U_\Xi^{(N)} = -18$ MeV.

$\Rightarrow$ Hyperons don't help

R. Nandi, P.C., S. Pal; PRC 99, 052802(R) (2019)

Mixed phase with quarks

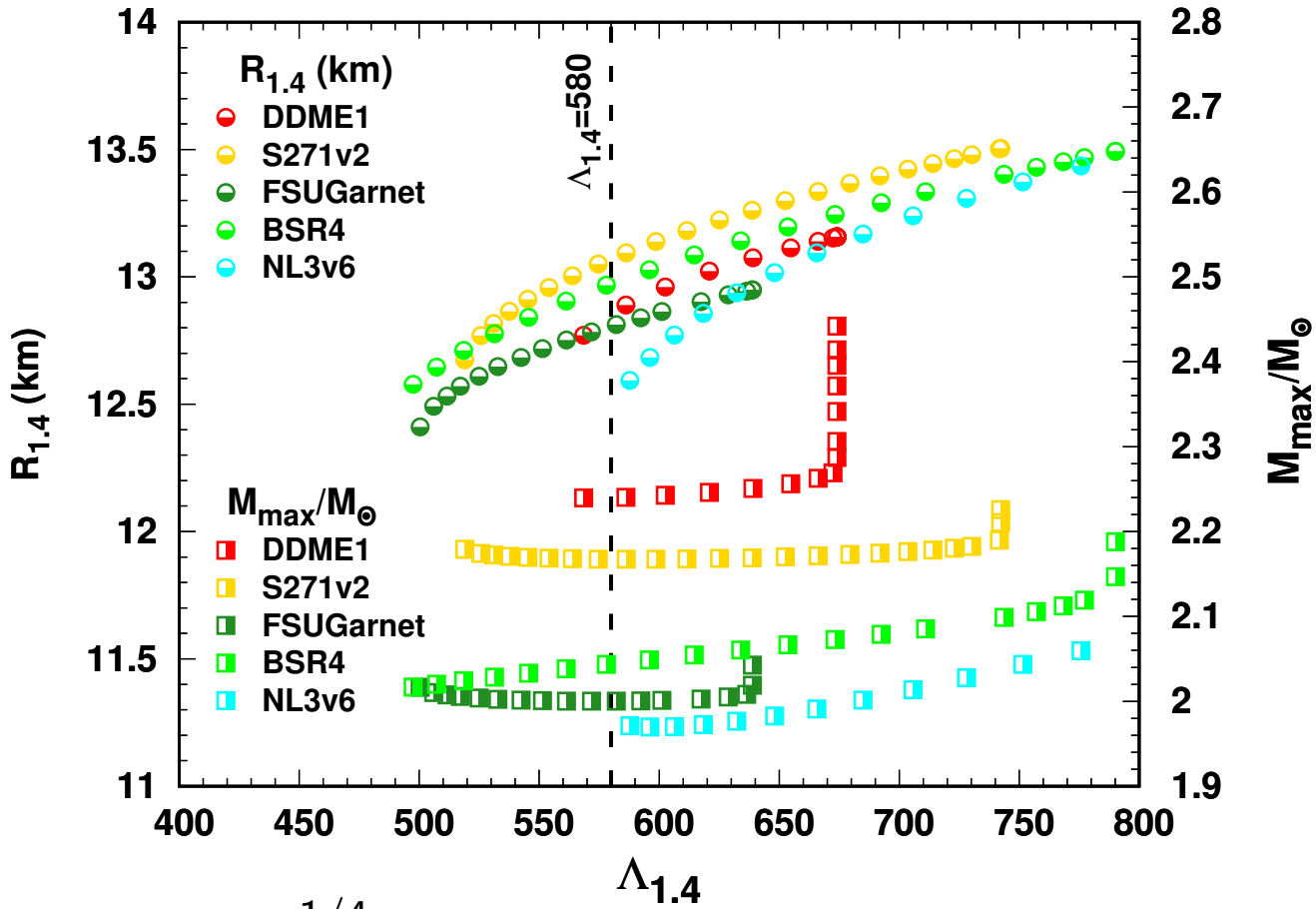

$B_{\rm eff}^{1/4}$ increases from left to right

R. Nandi, P.C., S. Pal, PRC 99, 052802(R) (2019); R. Nandi, S. Pal, EPJ ST 230, 551 (2021).

Hybrid Stars with Twins

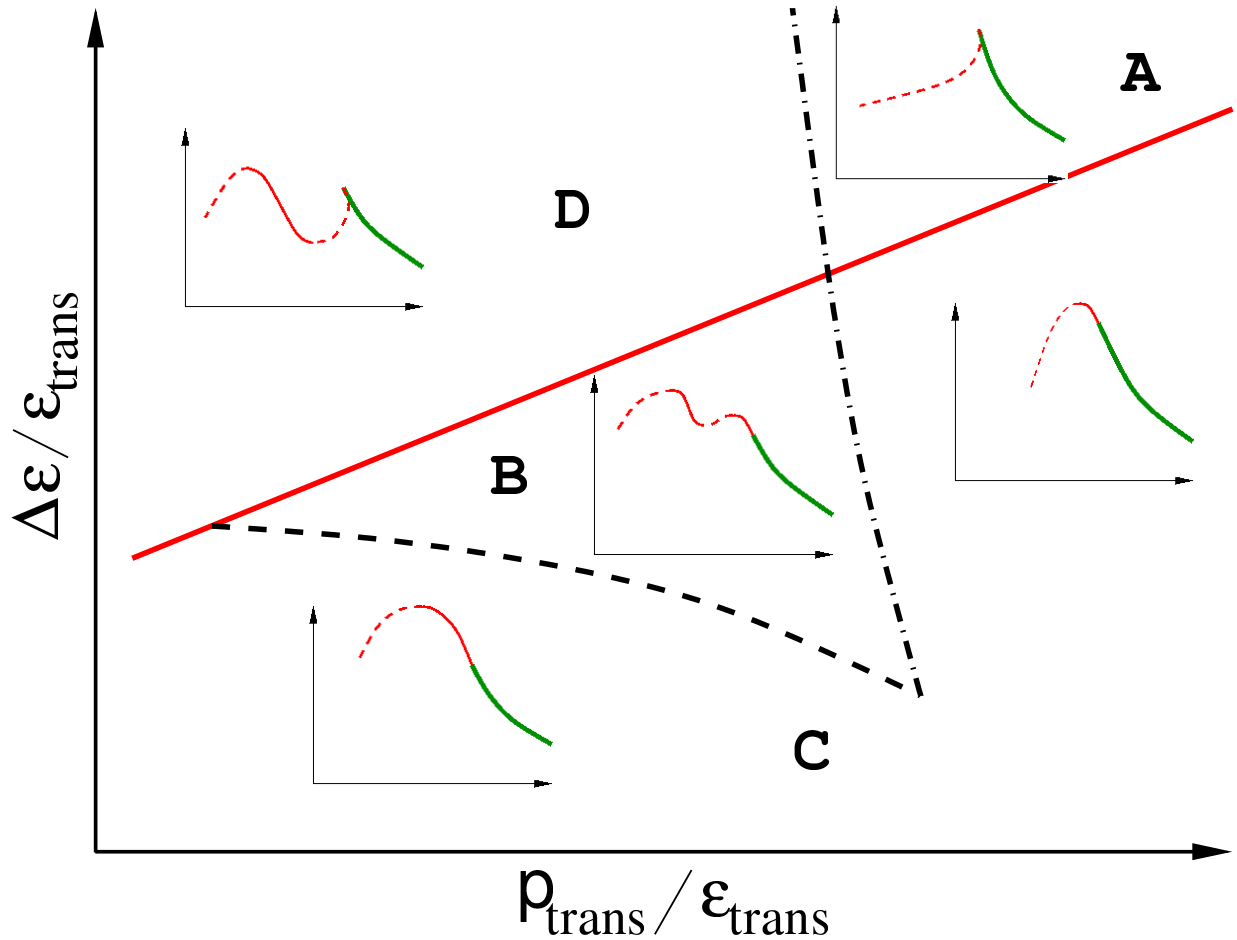

Alford et al., PRD 92 (2015) 083002

Two-Families Scenario

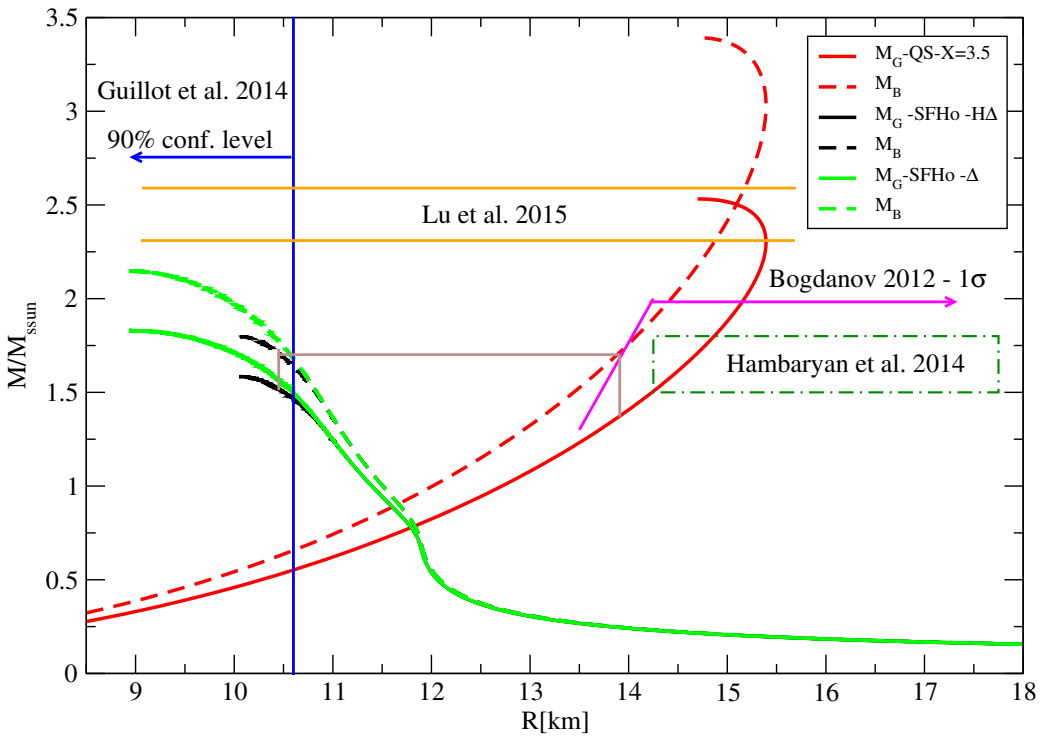

Drago et al., Eur.Phys.J. A52 (2016) 40

Main hypothesis:

- The ground state of nuclear matter is strange quark matter.
- Hadronic stars are metastable and under specific conditions, they convert into a strange quark star.
- Hadronic star and quark star would populate two separate branches.
- The heavier stars are the strange quark stars.

Agnostic approaches:

Generic parameterization of the EOS is preferred from an astrophysical perspective without too much model assumption.

- Piecewise polytropes: involves stitching of several adiabatic indices $\Gamma(\rho)$ for different range of densities.

  Read et al., PRD 79, 124032 (2009)

- Spectral parameterization: free parameters are the spectral indices which represent the adiabatic index $\Gamma(p) = \exp\left(\sum_k \gamma_k x^k\right)$, where $x \equiv \log(p/p_0)$ and p_0 is the pressure at half of nuclear saturation density.

  Lindblom, L. 2018, PhRvD, 97, 123019

- Nonparametric inference: estimation of EOSs using Gaussian processes.

  Landry and Essick, PRD, 99, 084049 (2019)

EOS inference:

- Given i different types of measurements and $j = 1, 2, \ldots, j(i)$ independent measurements of that type, then the likelihood of all of the data sets given EOS k is simply the product of the likelihoods:

$$\mathcal{L}_k = \prod_i \left[\prod_{j=1}^{j(i)} \mathcal{L}_k(i,j) \right] .$$

- Given the likelihood $\mathcal{L}_k$ of the full set of data for a specific EOS k, then in a Bayesian analysis the posterior probability P_k of the EOS is proportional to the prior probability q_k of the EOS times the likelihood:

$$P_k \propto q_k \mathcal{L}_k .$$

Latest NICER Findings:

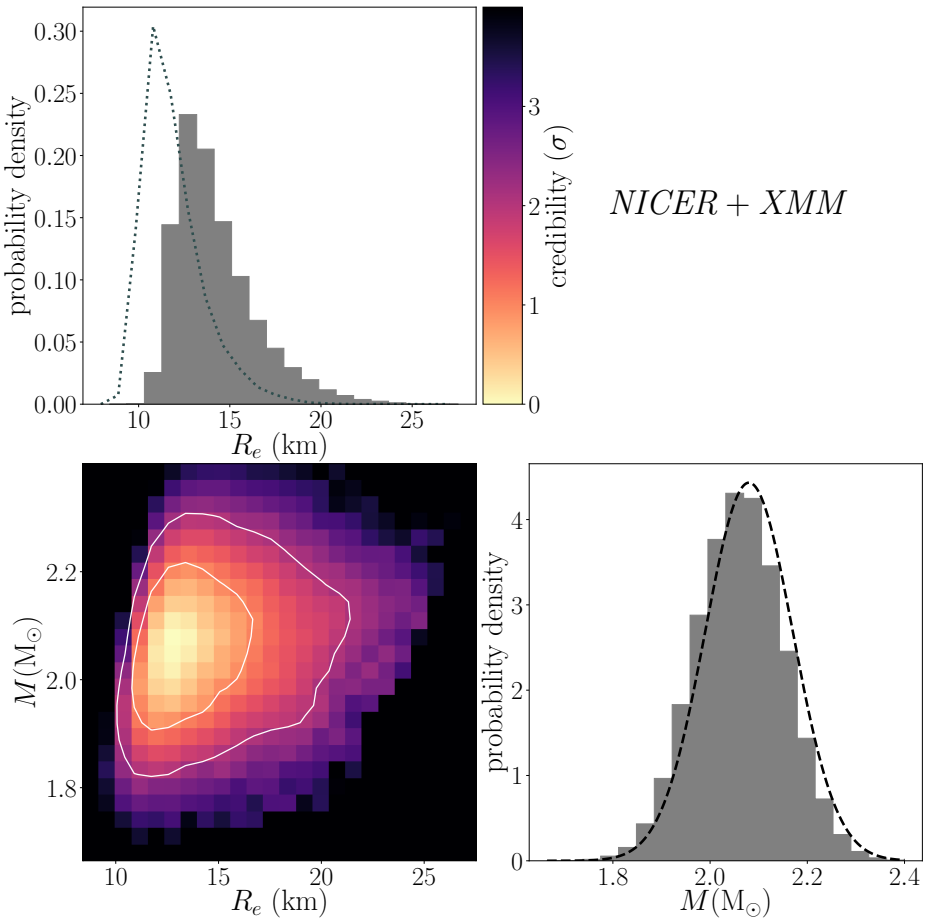

Figure: Simultaneous mass and radius measurements of J0740+6620 by NICER and XMM-Newton. (Miller et al., ApJL, 918, L28 (2021))

Latest NICER Findings: Constraints on the EOS

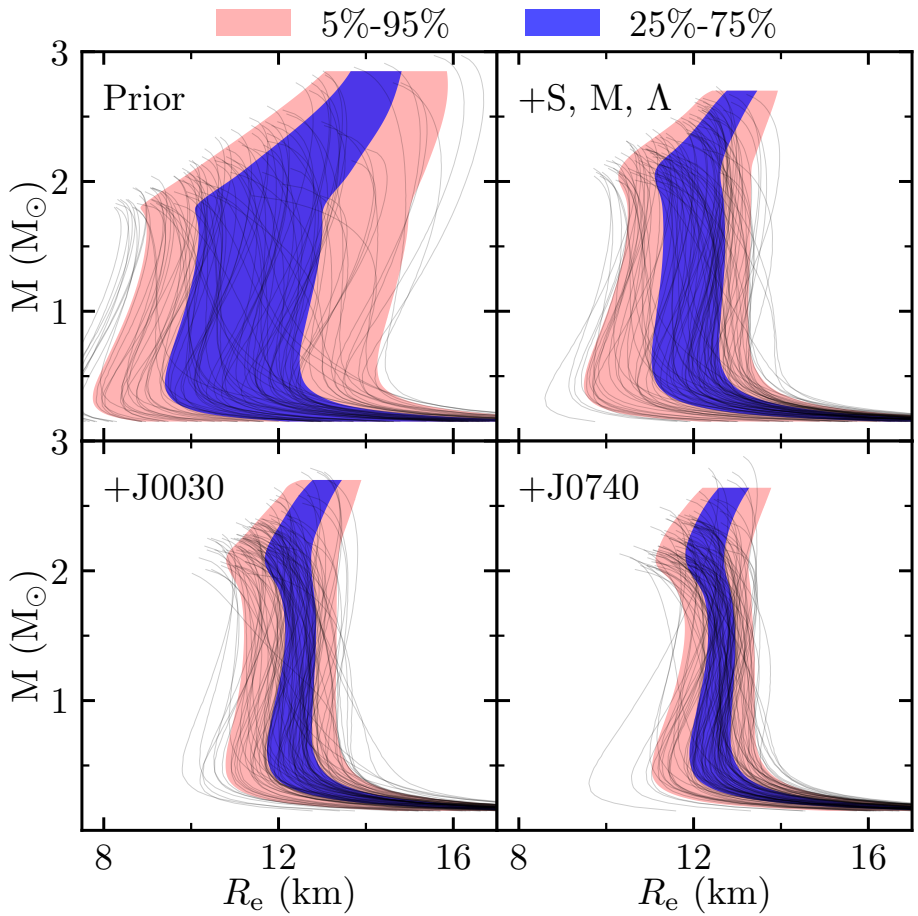

Figure: Effect of the combined constraints on the M-R plane. (Miller et al., ApJL, 918, L28 (2021))

Hints from Kilonovae:

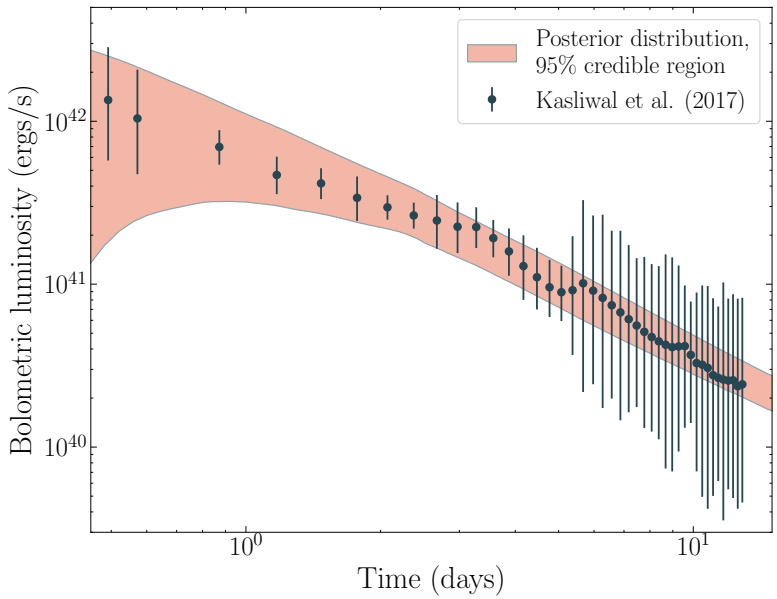

Figure: Bolometric Luminosity of GW170817

Two component kilonova model :

- dynamical ejecta
- neutrino driven wind

$\Rightarrow$

- Constraints on $q, \tilde{\Lambda}, M_{TOV}$

Raaijmakers et al., ApJL, 918, L29 (2021)

Further considerations

- Detection of GW190814 alters the game if the secondary object is taken to be a neutron star. If considered as a rapidly spinning NS, it would be the fastest rotating NS ever observed. However, without proper damping mechanism, it may have ended up a BH at some point of its evolution. This opens the possibility of constraining physical mechanisms, such as mutual friction in a superfluid interior.
- Constraints from neutron star cooling. The temperature measurements associated with direct or modified URCA processes can provide some indications on the composition of the core.
- Constraints from pulsar glitches. The phases of subsaturation inhomogeneous matter inside the inner crust region can be studied with pulsar glitches.

Summary:

- Any study of dense matter EOS is heavily model dependent. Therefore, a metamodelling approache to dense matter is very helpful to refine our knowledge.

- But, we have a promising future as more observations from NICER and future BNS detections will be able to pinpoint our understanding of the EOS.

Thank You